

Figure 12—Release profiles of pure and methylcellulose-treated hexobarbital from hard gelatin capsules in water with varying concentrations of polysorbate 80 at 37°. Key: open symbols, untreated drug; □, 0% polysorbate 80 ($\gamma_{LV} = 70.1$ dynes/cm); Δ, 0.01% (45.4 dynes/cm); ○, 0.05% (42.7 dynes/cm); ◇, 0.1% (41.4 dynes/cm); ▽, 0.2% (39.3 dynes/cm); ◊, 0.5% (37.7 dynes/cm); and *, 0.18% binder-treated drug in solutions with 0–0.5% polysorbate 80.

According to Finholt and Solvang (19), the surface tension of human gastric juice is nearly independent of pH and secretion rate, having a value between 35 and 50 dynes/cm. Therefore, a mean surface tension of human gastric juice of 43 dynes/cm would require a concentration of 0.05% polysorbate 80. To compare the release rates of pure and treated drug, the release profiles from capsules of hexobarbital, treated as described with a 3% methylcellulose solution and immersed in dissolution media of varying surface tension, are incorporated in Fig. 12. The results show the

release rate of the treated drug to be independent of the surface tension of the dissolution medium. Because of the aforementioned differences in the surface tension of human gastric juice, the realization of a release rate from capsules that is independent of the surface tension of the medium is of practical importance, especially where absorption is dissolution rate limited.

REFERENCES

- (1) A. H. Goldberg, M. Gibaldi, J. L. Kanig, and M. Mayersohn, *J. Pharm. Sci.*, **55**, 581 (1966).
- (2) W. L. Chiou and S. Riegelman, *ibid.*, **58**, 1505 (1969).
- (3) M. Gibaldi, S. Feldman, and T. R. Bates, *ibid.*, **60**, 1569 (1971).
- (4) R. K. Reddy, S. A. Khalil, and M. W. Gouda, *ibid.*, **65**, 1753 (1976).
- (5) J. M. Newton, G. Rowley, and J. F. V. Törnblom, *J. Pharm. Pharmacol.*, **23**, 156S (1971).
- (6) J. G. Allen and C. A. Davies, *ibid.*, **27**, 50 (1975).
- (7) S. Solvang and P. Finholt, *J. Pharm. Sci.*, **59**, 49 (1970).
- (8) D. E. Würster, *J. Am. Pharm. Assoc., Sci. Ed.*, **48**, 451 (1959).
- (9) R. E. Singiser and W. Lowenthal, *J. Pharm. Sci.*, **50**, 168 (1961).
- (10) H. C. Caldwell and E. Rosen, *ibid.*, **53**, 1387 (1964).
- (11) M. J. Robinson, G. M. Grass, and R. J. Lantz, *ibid.*, **57**, 1983 (1968).
- (12) E. J. de Jong, *Pharm. Weekbl.*, **104**, 469 (1969).
- (13) C. F. Lerk, A. J. M. Schoonen, and J. T. Fell, *J. Pharm. Sci.*, **65**, 843 (1976).
- (14) N. W. F. Kossen and P. M. Heertjes, *Chem. Eng. Sci.*, **20**, 593 (1965).
- (15) P. M. Heertjes and N. W. F. Kossen, *Powder Technol.*, **1**, 33 (1967).
- (16) W. C. Witvoet, Ph.D. thesis, Delft, The Netherlands, 1971.
- (17) J. B. Schwartz and T. P. Alvino, *J. Pharm. Sci.*, **65**, 572 (1976).
- (18) C. M. Hansen and P. E. Pierce, *Ind. Eng. Chem., Prod. Res. Develop.*, **13**, 218 (1974).
- (19) P. Finholt and S. Solvang, *J. Pharm. Sci.*, **57**, 1322 (1968).

ACKNOWLEDGMENTS

The authors thank Mrs. P. Broersma and Mr. K. Zuurman for technical assistance.

Kinetics of Aggregation of Human Platelets

ANWAR B. BIKHAZI** and GHASSAN E. AYYUB

Received May 25, 1977, from the School of Pharmacy, American University of Beirut, Beirut, Lebanon. Accepted for publication November 1, 1977. *Present address: Department of Physiology, School of Medicine, American University of Beirut, Beirut, Lebanon.

Abstract □ A study of the aggregation kinetics of human platelets using an electronic counting device is reported. The experimental data were analyzed quantitatively by a physical model, which assumed that the initial disappearance rate of single platelets versus time fitted a second-order type of aggregation with respect to platelet number. The mechanism of aggregation was surface barrier controlled. Thus, the aggregation rate constants in different adenosine diphosphate concentrations (1.5–9.0 μg) were 10–100 times greater than the rate constant (6.6325×10^{-12} cm³/sec) for a diffusion-controlled process as calculated from Smoluchowski's model. Also, the stability constant values, which were equal to unity in a fast diffusion-controlled mechanism, were smaller in the surface-barrier-controlled process and ranged from 0.00741 to 0.0467. The extent of aggregation was indicated by the calculation of a sticking probability constant as determined by the barrier. Adenosine

diphosphate induced a rapid aggregating effect. Prostaglandin E₁ produced the most drastic deaggregating effect as compared to dinoprostone (prostaglandin E₂) and dinoprost (prostaglandin F_{2α}). Aspirin completely blocked the aggregating effect of arachidonic acid.

Keyphrases □ Aggregation, platelet—kinetic study, effect of adenosine diphosphate, various prostaglandins, and arachidonic acid □ Kinetics—human platelet aggregation, effect of adenosine diphosphate, various prostaglandins, and arachidonic acid □ Adenosine diphosphate—effect on human platelet aggregation with and without various prostaglandins, kinetic study □ Prostaglandins, various—effect on human platelet aggregation with and without adenosine diphosphate, kinetic study □ Arachidonic acid—effect on human platelet aggregation with and without aspirin, kinetic study

The origin, morphology, chemical composition, lifespan, and role of some endogenous substances on blood coagulation and platelet aggregation have been reported (1–13).

Nevertheless, very few quantitative and mechanistic studies have been conducted on human platelet aggregation. The present study was an attempt to develop exper-

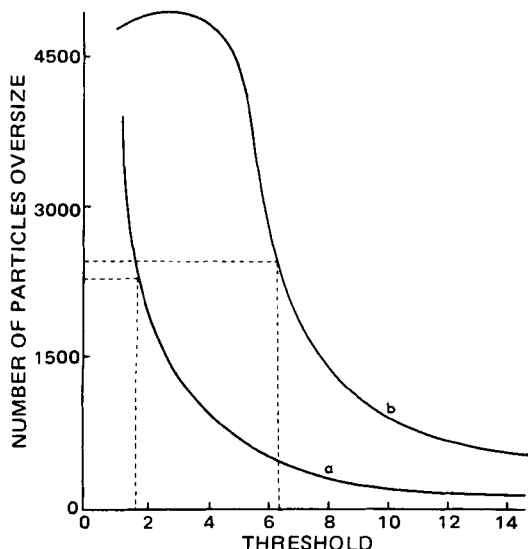


Figure 1—Cumulative size distribution plot of the number of particles oversize versus threshold for polyvinyltoluene-polystyrene latex calibration material. Key: a, 1.15- μm diameter latex; and b, 1.87- μm diameter latex.

imental techniques to provide data suitable for quantitative treatment and analysis.

EXPERIMENTAL

Particle Counting and Machine Calibration—An electronic counting device¹ was employed for platelet counting. According to estimates of platelet-size distribution (2–4 μm in diameter) (14), a 50- μm aperture opening tube was installed in the machine. Standard monosized calibration materials with a size range of 5–20% of the aperture diameter were used for calibration. The latex particles were dispersed in particle-free normal saline solution and placed on the counter stand for counting. The desired dilutions of the calibration material were made such that, at low threshold values (15), the machine would count at low coincidence factor.

Standard calibration curves were obtained when a plot of the number of particles oversize (15) versus threshold were drawn as shown in Figs. 1 and 2. The dotted lines in Figs. 1–4 indicate the threshold values corresponding to 50% of the number of particles in suspension (15) and, thus,

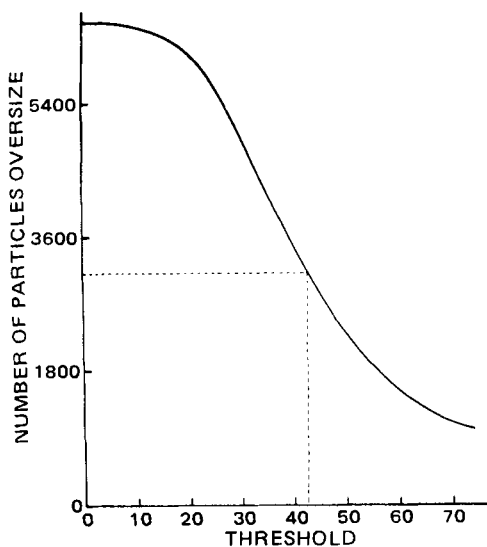


Figure 2—Cumulative size distribution plot of the number of particles oversize versus threshold for polystyrene-divinylbenzene latex of 5.02- μm diameter.

¹ Coulter counter model A, Coulter Electronics, Hialeah, Fla.

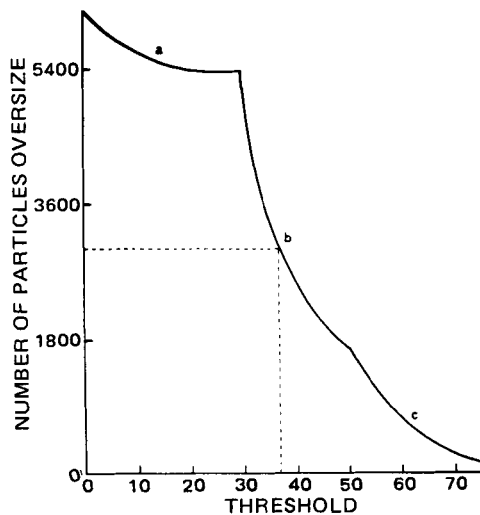


Figure 3—Cumulative size distribution plot of the number of particles oversize versus threshold for human blood cells. Key: a, size distribution for platelets; b, size distribution for red blood cells; and c, size distribution for white blood cells.

estimate the mean size distribution of particulate matter.

Preparation of Particle-Free Stock Solution—The particle-free stock solution was prepared as follows. Sodium chloride², 9 g, was dissolved in 1000 ml of distilled water. A stainless filter holder³, adapted with a 47-mm, 0.45- μm membrane filter³ and attached to a vacuum flask, was used for the filtration of the stock solution. The filtrate was refiltered until almost particle free as checked by the counter.

Part of the freshly prepared particle-free stock was used to fill the reservoir of the machine; this procedure was necessary to avoid leakage of particulate matter from the reservoir during flushing of the inner part of the aperture tube. Control studies were run in the following manner. The solution was poured into a clean beaker and then placed on the stand of the counter. Counts were recorded at specific threshold settings and were considered as background counts. The rest of the particle-free stock solution was used as suspending fluid for the calibration material and platelets.

Preparation of Platelet-Rich Plasma—Human blood was collected from the antecubital vein of healthy volunteers, 25–30 years old. The volunteers did not donate blood whenever they were under any type of drug therapy. To nine parts of blood, one part of 3.8% sodium citrate² was added. The mixture was then centrifuged⁴ at 77 \times g for 15 min. The su-

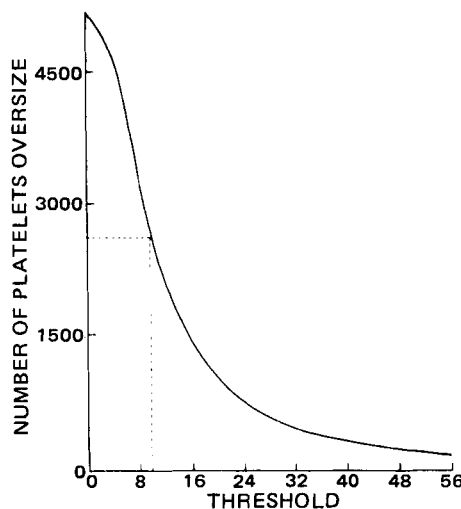


Figure 4—Cumulative size distribution plot of the number of platelets oversize versus threshold for human platelets in platelet-rich plasma.

² E. Merck, Darmstadt, Germany.

³ Millipore Corp., Bedford, Mass.

⁴ International clinical centrifuge model C.L., International Equipment Co., Needham, Mass.

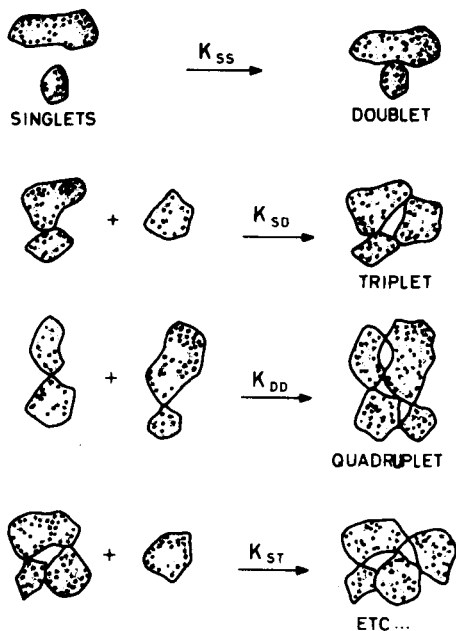


Figure 5—Proposed model for irreversible aggregation of human platelets.

pernatant platelet-rich plasma layer was collected. Then 0.5-ml samples of platelet-rich plasma were distributed into carefully cleaned 10-ml erlenmeyer flasks and placed in a water bath⁵ maintained at 37°.

Blood Particle Counts—After calibration of the counter, 2 μ l of human blood was injected into 80 ml of particle-free normal saline using a microliter syringe⁶. The suspended particles were stirred for 5 sec with a rotary glass stirrer attached to the counter. Counts were estimated per 0.05 ml of the suspension at different thresholds (Fig. 3).

Platelet Counts in Platelet-Rich Plasma—Twenty microliters of platelet-rich plasma was added to 80 ml of particle-free normal saline, and the number of platelets oversize *versus* threshold was estimated in a way similar to that used for blood particle counts (Fig. 4). The dotted lines in Fig. 4 show that threshold 9 was the setting for the average platelet size.

Control Experiments—Control experiments were regularly performed on every blood sample. A platelet-rich plasma sample was placed in an erlenmeyer flask in the water bath. Then 10 μ l of normal saline, which was used as a solvent for the compounds to be tested, was added to this control flask. Samples of 10 μ l were withdrawn at 0, 15, 30, 45, 60, 75, and 90 sec and added to 80 ml of normal saline to be counted.

Aggregation Experiments—At zero time, the test compounds were added with a microliter syringe to 0.5-ml platelet-rich plasma samples in a water bath at 37°. Sampling and analysis were done in exactly the same manner as described under *Platelet Counts in Platelet-Rich Plasma*. The compounds tested were prepared as follows.

The sodium salt of adenosine 5'-diphosphate⁷ was dissolved in normal saline in a concentration of 5 mg/5 ml. The stock solution was frozen, stored at -20°, and thawed when used.

Stock solutions of prostaglandin E₁⁸ and dinoprostone⁸ (prostaglandin E₂) were prepared by dissolving 2 mg in 0.02% sodium carbonate. The pH was adjusted to 7.35 with a pH meter⁹, and the final concentration of each prostaglandin was made up to 2 mg/10 ml with normal saline. Solutions were stored at -20° and thawed only when used.

A stock solution of dinoprost (prostaglandin F_{2 α}) tromethamine salt⁸ was prepared by dissolving a specific weight equivalent to 2 mg of dinoprost acid/10 ml of normal saline. The solution was stored at -20° and thawed only when used.

Arachidonic acid¹⁰ solution was prepared by dissolving 5 μ l of arachidonic acid in 0.3 ml of isotonic sodium chloride containing 0.02% sodium carbonate. The final concentration was 15 μ g/ μ l. The solution was stored at -20° and thawed only when used.

Aspirin² solution was prepared by dissolving 2.25 mg in 100 ml of normal saline for a final concentration of 2.25 μ g/10 μ l. The solution was stored at -20° and thawed only when used.

Calculations—Model—Figure 5 shows an irreversible particle-particle aggregation model for human platelets. The rate equations for the disappearance of singlets and for the formation of doublets, triplets, etc., may be written as:

$$\frac{d(P_s)}{dt} = -P_s(K_{ss}P_s + K_{sD}P_D + K_{sT}P_T + \dots) \quad (\text{Eq. 1})$$

$$\frac{d(P_D)}{dt} = K_{ss}P_s^2 - P_D(K_{sD}P_s + K_{DD}P_D + K_{DT}P_T + \dots) \quad (\text{Eq. 2})$$

$$\frac{d(P_T)}{dt} = K_{sD}P_sP_D - P_T(K_{sT}P_s + K_{DT}P_D + K_{TT}P_T + \dots) \quad (\text{Eq. 3})$$

where P_s , P_D , and P_T refer to singlet, doublet, and triplet counts, respectively; and K_{ss} , K_{sD} , K_{sT} , K_{DD} , K_{DT} , and K_{TT} are the rate constants of formation of doublets, triplets, and quadruplets. Similar equations can be written for higher aggregates.

Assumptions—

1. Human platelets were assumed to be monodispersed and spherical in shape.

2. The rate constants in the equations were assumed to be equal, thus simplifying the solution of the system of differential equations (16).

3. The experiments were concerned with the initial rapid aggregation of singlets; therefore, the formation rates of triplets and higher aggregates were not being kinetically measured. For this reason, platelets during the experiments were measured at threshold 9 of the machine, corresponding to the number of singlets existing at any time in the platelet-rich plasma sample.

Diffusion-Controlled Case—The rigorous aggregation expression for a monodispersed system was proposed by Smoluchowski (16). If it is assumed that platelets are spherical in nature, then:

$$\frac{d \sum_{k=1}^{\infty} P_k}{dt} = -\frac{1}{2} \sum_{i=1}^{\infty} \sum_{j=1}^{\infty} \frac{4\pi D_{ij} r_{ij} P_i P_j}{W_{ij}} \quad (\text{Eq. 4})$$

where D_{ij} is the mutual diffusivity of the i th and j th class particles; r_{ij} is the collision radius; W_{ij} is the stability constant; and P_k , P_i , and P_j are platelet counts in classes k , i , and j , respectively. If platelets are assumed to be monodispersed, then the mutual diffusivity, D_{ij} , of two platelets is equal to the sum of the diffusivities of each individual platelet:

$$D_{ij} = D_i + D_j = 2D_i = 2D_s \quad (\text{Eq. 5})$$

and:

$$r_{ij} = r_i + r_j = 2r_i = 2r_s \quad (\text{Eq. 6})$$

where D_s and r_s are the diffusivity and radius of a singlet, respectively. Then:

$$K_{ij} = K_{ss} = \frac{4\pi(D_i + D_j)(r_i + r_j)}{W_{ij}} = \frac{16\pi D_s r_s}{W} \quad (\text{Eq. 7})$$

The Stokes-Einstein relation defines the diffusivity as:

$$D_s = \frac{K_0 T}{6\pi n r_s} \quad (\text{Eq. 8})$$

where K_0 is the Boltzmann constant, T is the absolute temperature, and n is the viscosity of the medium. Combining Eqs. 7 and 8 and substituting for D_s yield:

$$K_{ss} = \frac{8K_0 T}{3nW} \quad (\text{Eq. 9})$$

For a monodispersed system, Eqs. 1 and 4 can be combined to give:

$$\frac{d(P_s)}{dt} = -K_{ss}(P_s)^2 \quad (\text{Eq. 10})$$

By substituting Eq. 9 into Eq. 10 and integrating, the following expression is obtained:

$$\frac{1}{P_s} = \frac{1}{P_{s0}} + K_{ss}t = \frac{1}{P_{s0}} + \frac{8K_0 T}{3nW} t \quad (\text{Eq. 11})$$

where P_{s0} is the number of singlets at time zero. Equation 11 includes the rate constant K_{ss} for diffusion-controlled aggregation, *i.e.*, when $W = 1$. Thus, K_{ss} has a value of 6.6325×10^{-12} cm³/sec at 37° for human platelets suspended in plasma having a viscosity equal to 0.0172 poise (17). The value of $W > 1$ explains the experimental deviation of a system from a rapidly aggregating diffusion-controlled process. Instances where

⁵ Thermocirculator model 1818, Beckman Instruments, Fullerton, Calif.

⁶ Hamilton Co., Reno, Nev.

⁷ Koch-Light Laboratories, Colnbrook Brecks, England.

⁸ The Upjohn Co., Kalamazoo, Mich.

⁹ Expandomatic SS-2, Beckman Instruments, Fullerton, Calif.

¹⁰ Sigma Chemical Co., St. Louis, Mo.

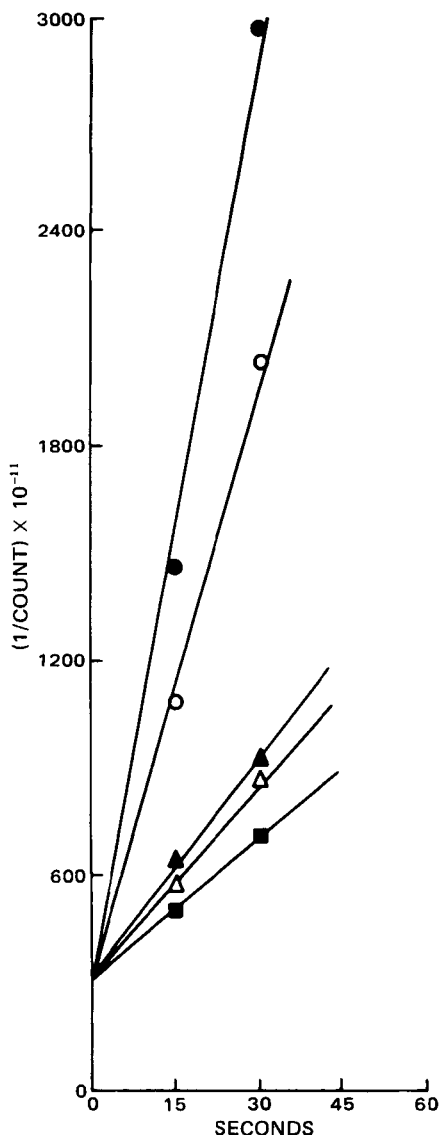


Figure 6—Plot of $1/\text{platelet count}$ versus time for platelet aggregation as induced by adenosine diphosphate. Key (concentrations of adenosine diphosphate per milliliter of platelet-rich plasma): ■, 1.5 μg ; ▲, 3 μg ; ▲, 4.5 μg ; ○, 6 μg ; and ●, 9 μg .

$W < 1$ (18) also can apply for a rapid aggregation process. The half-life of singlet aggregation under the influence of a diffusion-controlled process is calculated from Eq. 11 to be:

$$t_{1/2} = \frac{1}{P_{s0}K_{ss}} = \frac{3nW}{8P_{s0}K_0T} \quad (\text{Eq. 12})$$

Surface-Barrier-Controlled Case—Higuchi *et al.* (19) proposed that the rate constant K_{ss} includes the total available surface area of contact between two singlets:

$$K_{ss} = (\text{total available contact area})(D_s + D_s)(\gamma) \quad (\text{Eq. 13})$$

Table I—Rate Constants, Half-Lives, and Sticking Probability Factors of Platelet Aggregation in the Presence of Adenosine Diphosphate

Adenosine Diphosphate ^a , μg	Rate Constant ^b , $K_{ss} \times 10^{-11}$, cm^3/sec	Half-Life, $t_{1/2}$, sec	Sticking Probability Factor, $\gamma \times 10^6/\text{cm}/\text{Platelet}$
1.5	14.20	21.47	0.0993
3.0	19.50	15.64	0.1364
4.5	21.40	14.24	0.1496
6.0	57.56	5.30	0.4025
9.0	89.50	3.40	0.6259

^a Amount injected into 1 ml of platelet-rich plasma. ^b Rate constant is zero for control experiment.

Table II—Rate Constants, Half-Lives, and Sticking Probability Factors of Platelet Aggregation in the Presence of Adenosine Diphosphate and Prostaglandin E_1

Adenosine Diphosphate ^a , μg	Prostaglandin E_1 ^a , μg	Rate Constant ^b , $K_{ss} \times 10^{-11}$, cm^3/sec	Half-Life, $t_{1/2}$, sec	Sticking Probability Factor, $\gamma \times 10^6/\text{cm}/\text{Platelet}$
3.0	0.0	19.50	15.64	0.1364
3.0	0.06	5.20	58.65	0.0363
6.0	0.0	57.56	5.30	0.4025
6.0	0.12	3.88	78.61	0.0271
9.0	0.0	89.50	3.40	0.6259
9.0	0.18	1.03	296.12	0.0072

^a Amount injected into 1 ml of platelet-rich plasma. ^b Rate constant is zero for control experiments.

where γ , a constant for a given system in which the local curvatures of the contacting surfaces are identical, includes the sticking probability as determined by the barrier. For singlet-singlet interacting particles in a monodispersed system, the total available contacting area for spheres is $16\pi r_s^2$. Then Eq. 13 is written as:

$$K_{ss} = 32\pi r_s^2 D_s \quad (\text{Eq. 14})$$

Substituting in Eq. 14 for D_s gives:

$$K_{ss} = \frac{16\gamma K_0 r_s T}{3n} \quad (\text{Eq. 15})$$

Thus, Eq. 10 can be evaluated as:

$$\frac{d(P_s)}{dt} = -\frac{16\gamma K_0 r_s T}{3n} (P_s)^2 \quad (\text{Eq. 16})$$

The integrated form of Eq. 16 is written as:

$$\frac{1}{P_s} = \frac{1}{P_{s0}} + \frac{16\gamma K_0 r_s T}{3n} t \quad (\text{Eq. 17})$$

The rate constant in Eq. 17 is the surface-barrier-controlled rate constant. Any change in the surface barrier is explained by the difference of the sticking probability factor, γ , which is used to determine the degree of the surface-barrier effect on the aggregation of human platelets. From Eq. 17, the half-life of the aggregated particles under the surface-barrier-controlled processes is equal to:

$$t_{1/2} = \frac{1}{P_s K_{ss}} = \frac{3n}{16P_s K_0 r_s T \gamma} \quad (\text{Eq. 18})$$

RESULTS

Counter Calibration—Figures 1 and 2 represent calibration curves for calibration material of sizes 1.87, 1.15, and 5.02 μm . The results were employed for the quantitative estimates of human blood cell sizes and human platelet size.

Size Distribution of Human Blood Cells—Figure 3 shows the size distribution of human blood cells. Particulate matter in whole blood was not narrowly distributed. There were approximately three different size distributions, as shown by breaks in the curve. This result was explained on the basis of the differences in the size distributions of platelets, red blood cells, and white blood cells. The machine setting, when counting whole blood cells, differed from that when counting platelets alone (Figs.

Table III—Rate Constants, Half-Lives, and Sticking Probability Factors of Platelet Aggregation in the Presence of Adenosine Diphosphate and Dinoprostone

Adenosine Diphosphate ^a , μg	Dinoprostone ^a , μg	Rate Constant ^b , $K_{ss} \times 10^{-11}$, cm^3/sec	Half-Life, $t_{1/2}$, sec	Sticking Probability Factor, $\gamma \times 10^6/\text{cm}/\text{Platelet}$
3.0	0.0	19.50	15.64	0.1364
3.0	0.6	10.60	28.77	0.0741
6.0	0.0	57.56	5.30	0.4025
6.0	1.2	18.75	16.27	0.1311
9.0	0.0	89.50	3.40	0.6259
9.0	1.8	36.80	8.29	0.2573

^a Amount injected into 1 ml of platelet-rich plasma. ^b Rate constant is zero for control experiments.

Table IV—Rate Constants, Half-Lives, and Sticking Probability Factors of Platelet Aggregation in the Presence of Adenosine Diphosphate and Dinoprost

Adenosine Diphosphate ^a , μg	Dinoprost ^a , μg	Rate Constant ^b , $K_{ss} \times 10^{-11}$, cm^3/sec	Half-Life, $t_{1/2}$, sec	Sticking Probability Factor, $\gamma \times 10^6/\text{cm}/\text{Platelet}$
3.0	0.0	19.50	15.64	0.1364
3.0	0.6	13.76	22.16	0.0962
6.0	0.0	57.56	5.30	0.4025
6.0	1.2	21.20	14.38	0.1482
9.0	0.0	89.50	3.40	0.6259
9.0	1.8	34.57	8.82	0.2417

^a Amount injected into 1 ml of platelet-rich plasma. ^b Rate constant is zero for control experiments.

1 and 2). Thus, it was difficult to approximate the average size of human platelets from the a portion in Fig. 3.

Size Distribution of Particles in Platelet-Rich Plasma—Figure 4 represents the size distribution of platelets in platelet-rich plasma. The plot showed a narrow size distribution of platelets. From Figs. 1 and 4, the average diameter of human platelets was calculated to be around 2.15 μm .

Control Studies—These studies were carried out to check the effect of simulating the experimental situations in the absence of an aggregating or deaggregating agent on platelets. Under all experimental conditions, the amount of sodium chloride available in a specific volume of normal saline (10 or 20 μl) injected into 1 ml of platelet-rich plasma had no effect on platelet aggregation. Since control runs for all systems studied showed no aggregation, a plot of 1/platelet count versus threshold would show a horizontal line with a slope of zero.

Effect of Adenosine Diphosphate on Platelet Aggregation—Figure 6 shows a plot of 1/platelet count versus time in seconds on the effect of different concentrations (1.5, 3.0, 4.5, 6.0, and 9.0 $\mu\text{g}/\text{ml}$ of platelet-rich plasma) of adenosine diphosphate on platelet aggregation. The data points were only for the first 30 sec; the results (Table I) showed linearity with all adenosine diphosphate concentrations, agreeing with the theory of Eqs. 10 and 16. With an increase in adenosine diphosphate concentration, the aggregation rate increased drastically.

Effect of Prostaglandins on Platelet Aggregation without and with Adenosine Diphosphate—*Prostaglandin E₁ Alone*—Aggregation was not observed with 0.2 and 0.4 μg of prostaglandin E₁/ml of platelet-rich plasma. Slight deaggregation occurred with platelets originally in

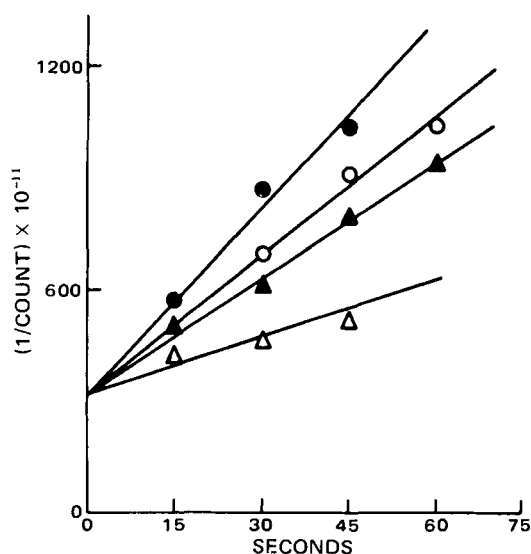


Figure 7—Plot of 1/platelet count versus time for platelet aggregation showing the effect of prostaglandins on adenosine diphosphate-induced platelet aggregation. Key (concentrations per milliliter of platelet-rich plasma): ●, 3 μg of adenosine diphosphate; ○, 3 μg of adenosine diphosphate and 0.6 μg of dinoprost; ▲, 3 μg of adenosine diphosphate and 0.6 μg of dinoprostone; and △, 3 μg of adenosine diphosphate and 0.06 μg of prostaglandin E₁.

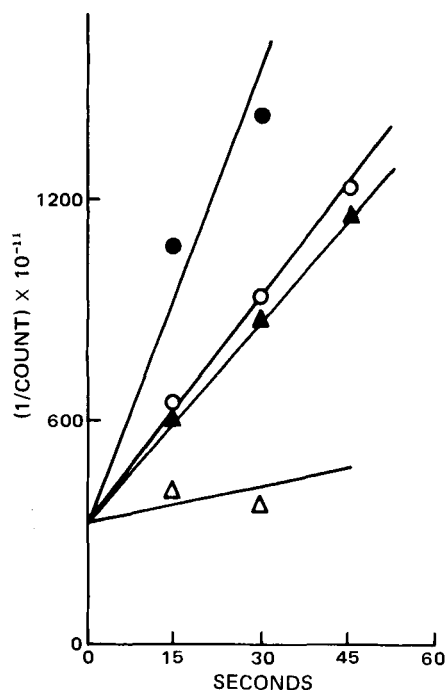


Figure 8—Plot of 1/platelet count versus time for platelet aggregation showing the effect of prostaglandins on adenosine diphosphate-induced platelet aggregation. Key (concentrations per milliliter of platelet-rich plasma): ●, 6 μg of adenosine diphosphate; ○, 6 μg of adenosine diphosphate and 1.2 μg of dinoprost; ▲, 6 μg of adenosine diphosphate and 1.2 μg of dinoprostone; and △, 6 μg of adenosine diphosphate and 0.12 μg of prostaglandin E₁.

the aggregated state. This result is consistent with the results of the platelet-size distribution (Fig. 4), which did not rule out the possibility of platelets being partly aggregated in the platelet-rich plasma sample.

Dinoprostone Alone—With dinoprostone at 1.0, 2.0, and 4.0 $\mu\text{g}/\text{ml}$ of platelet-rich plasma, neither aggregation nor deaggregation of human platelets occurred.

Dinoprost Alone—Dinoprost tromethamine in amounts equivalent to 1.0, 2.0, and 4.0 μg of dinoprost/ml of platelet-rich plasma did not cause aggregation or deaggregation.

Prostaglandin E₁ with Adenosine Diphosphate—Three different concentrations of adenosine diphosphate and prostaglandin E₁ were added per milliliter of platelet-rich plasma to induce aggregation. The concentrations were 3.0 μg of adenosine diphosphate and 0.06 μg of prostaglandin E₁, 6.0 μg of adenosine diphosphate and 0.12 μg of prostaglandin E₁, and 9.0 μg of adenosine diphosphate and 0.18 μg of prostaglandin E₁.

Table II shows the results observed for adenosine diphosphate inducing aggregation without and with prostaglandin E₁. Prostaglandin E₁ induced a deaggregating effect. For example, at 3.0 μg of adenosine diphosphate, the aggregation rate constant was calculated to be $1.95 \times 10^{-10} \text{ cm}^3/\text{sec}$; in the presence of 0.06 μg of prostaglandin E₁, the rate constant was reduced to $5.2 \times 10^{-11} \text{ cm}^3/\text{sec}$. This result was similarly observed at 6.0 and 9.0 μg of prostaglandin E₁/ml of platelet-rich plasma. Prostaglandin E₁ had a drastic effect on platelet deaggregation, even in the presence of a strong aggregating agent like adenosine diphosphate.

Dinoprostone with Adenosine Diphosphate—Three different concentrations of adenosine diphosphate and dinoprostone were added per milliliter of platelet-rich plasma. The concentrations were 3.0 μg of adenosine diphosphate and 0.6 μg of dinoprostone, 6.0 μg of adenosine diphosphate and 1.2 μg of dinoprostone, and 9.0 μg of adenosine diphosphate and 1.8 μg of dinoprostone. Table III shows a deaggregating effect of dinoprostone on adenosine diphosphate-induced platelet aggregation. The effect was not as drastic as with prostaglandin E₁, although the amount of prostaglandin E₁ was 10 times less than that of dinoprostone.

Dinoprost Tromethamine with Adenosine Diphosphate—The concentrations of adenosine diphosphate and dinoprost were similar to those used for studying the effect of adenosine diphosphate and dinoprostone. As shown in Tables III and IV, dinoprost had an effect similar to that of

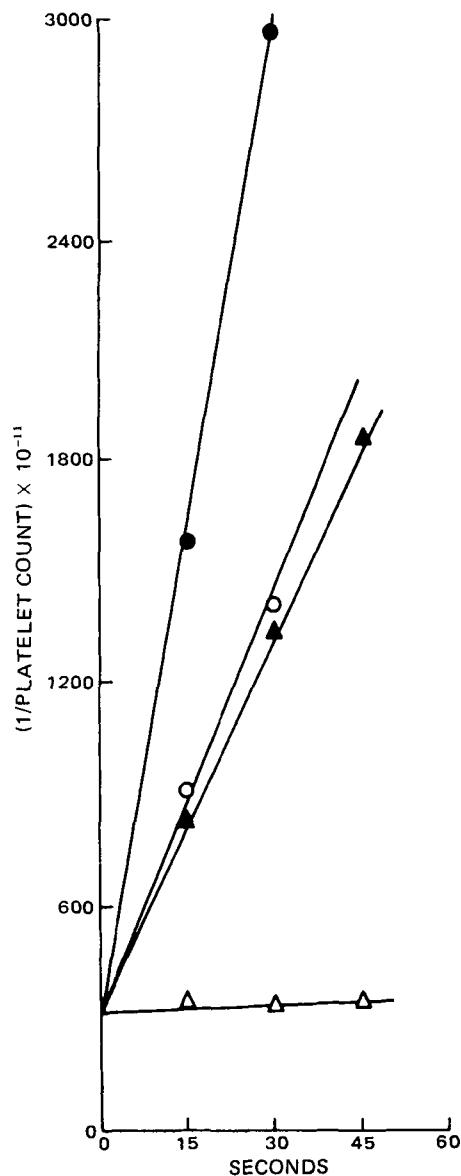


Figure 9—Plot of 1/platelet count versus time for platelet aggregation showing the effect of prostaglandins on adenosine diphosphate-induced platelet aggregation. Key (concentrations per milliliter of platelet-rich plasma): ●, 9 µg of adenosine diphosphate; ○, 9 µg of adenosine diphosphate and 1.8 µg of dinoprostone; ▲, 9 µg of adenosine diphosphate and 1.8 µg of dinoprost; and △, 9 µg of adenosine diphosphate and 0.18 µg of prostaglandin E₁.

dinoprostone on adenosine diphosphate-induced platelet aggregation.

Figures 7–9 are comparative plots of 1/platelet count versus time on rectangular coordinates, showing the effect of the prostaglandins on platelet aggregation as induced by adenosine diphosphate. Prostaglandin E₁ had the strongest effect followed by dinoprostone and dinoprost. Table V shows the extent of the effect of each prostaglandin on platelet aggregation in the presence of adenosine diphosphate.

Effect of Arachidonic Acid and Aspirin on Platelet Aggregation—Arachidonic acid, a well-known precursor (20) in the biosynthesis of dinoprostone and dinoprost, showed no effect on platelet aggregation at 90, 180, and 360 µg/ml of platelet-rich plasma. But at 540 and 720 µg/ml of platelet-rich plasma, an aggregating effect was observed. The addition of 2.25 µg of aspirin/ml of platelet-rich plasma appeared to block the aggregating effect of arachidonic acid (Fig. 10). This concentration of aspirin was far lower than a sustained blood level concentration for a patient continuously taking 600 mg of the drug three times daily. Table VI shows the rate constants, sticking probability factor, and half-life of the effect of arachidonic acid on platelet aggregation in the absence and presence of aspirin.

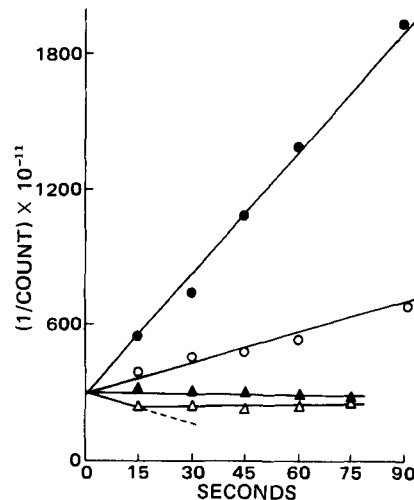


Figure 10—Plot of 1/platelet count versus time of platelet aggregation showing the effect of arachidonic acid in the absence and presence of aspirin. Key (concentrations per milliliter of platelet-rich plasma): ○, 540 µg of arachidonic acid; ●, 720 µg of arachidonic acid; △, 540 µg of arachidonic acid and 2.25 µg of aspirin; and ▲, 720 µg of arachidonic acid and 2.25 µg of aspirin.

DISCUSSION

The present approach emphasizes a physical or kinetic description of platelet aggregation and introduces a quantitative method for measuring the aggregation rate of human platelets *in vitro*. This method has one major advantage over the turbidimetric method (9), namely, its sensitivity. The experiments were carried out only for a few minutes, and sampling was done within 15-sec intervals for a series of experiments. Thus, the emphasis was on the initial rate of platelet aggregation utilizing a simplified model (Fig. 5 and Eqs. 11 and 17). Higher order aggregation or deaggregation occurring at longer times is complex, and analysis of the higher order interactions was not attempted. This complexity was apparent in the data obtained after approximately 1-min intervals.

The described process of platelet aggregation most probably occurs by a surface-barrier-controlled mechanism. This hypothesis is, with adenosine diphosphate for example, supported by larger values of the rate constants ranging from 1.42×10^{-10} to 8.95×10^{-10} cm³/sec as compared to 6.6325×10^{-12} cm³/sec for the Smoluchowski approach. The values of these rate constants for the other systems varied from around 10- to 100-fold higher as compared with the rate constant for a diffusion-controlled process (Table V).

It is concluded that platelets suspended in plasma (viscosity of human plasma is 0.0172 poise at 37°) have a low probability of moving under their diffusivities and, thus, aggregating. By calculating the diffusivity of a human platelet with the Stokes–Einstein equation (Eq. 8), a value of 1.226

Table V—Compilation of Rate Constants, Half-Lives, and Sticking Probability Factors of Platelet Aggregation in the Presence of Adenosine Diphosphate and Prostaglandins

Adenosine Diphosphate ^a , µg	Prostaglandin ^a , µg	Rate Constant ^b , K _{ss} × 10 ⁻¹¹ , cm ³ /sec	Half-Life, t _{1/2} , sec	Sticking Probability Factor, γ × 10 ⁶ /cm/Platelet
3.0	0.0	19.50	15.64	0.1364
3.0	0.06 ^c	5.20	58.65	0.0363
3.0	0.6 ^d	10.60	28.77	0.0741
3.0	0.6 ^e	13.76	22.16	0.0962
6.0	0.0	57.56	5.30	0.4025
6.0	0.12 ^c	3.88	78.61	0.0271
6.0	1.2 ^d	18.75	16.27	0.1311
6.0	1.2 ^e	21.20	14.38	0.1482
9.0	0.0	89.50	3.40	0.6259
9.0	0.18 ^c	1.03	296.12	0.0072
9.0	1.8 ^d	36.80	8.29	0.2573
9.0	1.8 ^e	34.57	8.82	0.2417

^a Amount injected into 1 ml of platelet-rich plasma. ^b Rate constant is zero for control experiments. ^c Results for prostaglandin E₁. ^d Results for dinoprostone. ^e Results for dinoprost.

Table VI—Rate Constants, Half-Lives, and Sticking Probability Factors of Platelet Aggregation in the Presence of Arachidonic Acid and Aspirin

Arachidonic Acid ^a , μg	Aspirin ^a , μg	Rate Constant ^b , $K_{ss} \times 10^{-11}$, cm^3/sec	Half-Life, $t_{1/2}$, sec	Sticking Probability Factor, $\gamma \times 10^6/\text{cm}/\text{Platelet}$
540	0.0	3.18	95.90	0.0222
720	0.0	18.90	16.10	0.1321
540	2.25	-0.24	—	-0.0016
720	2.25	-4.40	—	-0.0307

^a Amount injected into 1 ml of platelet-rich plasma. ^b Rate constant is zero for control experiments.

$\times 10^{-9} \text{ cm}^2/\text{sec}$ is obtained, which is rather small compared to molecular diffusivities which are usually about 10^{-4} – $10^{-6} \text{ cm}^2/\text{sec}$. Platelets physically approaching each other may be repulsed or aggregated or aggregates may disperse, depending on the reactivity of their surfaces, which is modulated by the molecular species in the solution.

The surface-barrier process is further supported by calculated values of the stability constant, W , from Eq. 9 showing numbers smaller than 1. Values of the sticking probability constant, γ , were calculated and are reported in Tables I–VI. As reported previously (10), adenosine diphosphate produces an alteration in the platelet membrane surface. Therefore, larger γ values in the presence of adenosine diphosphate probably are the result of a specific modification of the membrane surface reactivity by that compound. More work is needed regarding the biosynthesis of prostaglandins and surface-barrier effects.

The experimental results with prostaglandins and aspirin suggest the following with respect to therapeutics. If it is assumed that the blood volume in an average individual is 5 liters and that a person receiving aspirin or prostaglandin has complete systemic availability of the dose with little or no tissue distribution, the doses of aspirin and prostaglandin E_1 needed to block platelet aggregation completely will be around 10 and 1 mg, respectively. Thus, a combined dose of aspirin and prostaglandin E_1 will have a dual effect in blocking platelet aggregation and possibly thrombus formation.

REFERENCES

(1) E. J. W. Bowle, J. H. Thompson, and C. A. Owen, *Mayo Clin. Proc.*, **40**, 625 (1965).

- (2) J. H. Wright, *J. Morphol.*, **21**, 263 (1910).
 (3) W. H. Howell and D. D. Donahue, *J. Exp. Med.*, **65**, 177 (1937).
 (4) E. Fidler and E. T. Waters, *ibid.*, **73**, 299 (1941).
 (5) B. N. Erickson, H. H. Williams, I. Avrin, and P. Lee, *J. Clin. Invest.*, **18**, 81 (1939).
 (6) K. A. Aas and F. H. Gardner, *ibid.*, **37**, 1257 (1958).
 (7) A. Gaarder, J. Jonsen, S. Loland, and D. Hellem, *Nature (London)*, **129**, 531 (1961).
 (8) R. L. Vigdahl, N. R. Marquis, and P. A. Tavormina, *Biochem. Biophys. Res. Commun.*, **37**, 409 (1969).
 (9) D. J. Bouillin, R. A. Green, and S. K. Price, *J. Physiol.*, **221**, 415 (1972).
 (10) E. W. Salzman, *N. Engl. J. Med.*, **286**, 358 (1972).
 (11) S. Bergstrom, H. Danielsson, and B. Samuelsson, *Biochim. Biophys. Acta*, **90**, 204 (1964).
 (12) M. J. Silver, W. Hoch, J. J. Kocsis, and G. M. Ingerman, *Science*, **183**, 1085 (1974).
 (13) U. S. Van Euler, F. Dray, and S. M. M. Karim, "Prostaglandins in Documenta Geigy," Ciba-Geigy Ltd., Basel, Switzerland, 1974.
 (14) M. M. Wintrobe, "Blood Platelets and Coagulation in Clinical Hematology," 6th ed., Lea & Febiger, Philadelphia, Pa., 1967.
 (15) A. B. Bikhazi, J. A. Shiaty, and A. F. Haddad, *J. Pharm. Sci.*, **66**, 181 (1977).
 (16) H. R. Kruyt, "Colloid Science," vol. 1, Elsevier, Amsterdam, The Netherlands, 1952.
 (17) G. E. Ayyub, M.S. thesis, American University of Beirut, Beirut, Lebanon, 1976.
 (18) D. F. Bernstein, Ph.D. dissertation, University of Michigan, Ann Arbor, Mich., 1971.
 (19) W. I. Higuchi, R. Okada, G. A. Stelter, and A. P. Lemberger, *J. Pharm. Sci.*, **52**, 49 (1963).
 (20) B. B. Vargaftig and P. Zirinis, *Nature New Biol.*, **224**, 114 (1973).

ACKNOWLEDGMENTS

Presented at the Basic Pharmaceutics Section, APhA Academy of Pharmaceutical Sciences, New York meeting, May 1977.

Supported in part by a grant from the University Medical Research Fund, American University of Beirut, Beirut, Lebanon.

The authors thank The Upjohn Co., Kalamazoo, Mich., for providing samples of prostaglandins.

Possible Ion-Pair-Mediated Absorption of Mixidine I: Partitioning and Lethality Studies

W. DOUGLAS WALKLING *, ANTOINETTE C. BONFILIO, and HENRY I. JACOBY

Received August 12, 1977, from the *Research Division, McNeil Laboratories, Inc., Fort Washington, PA 19034.* Accepted for publication October 28, 1977.

Abstract □ Mixidine, a very soluble base which is completely ionized in all physiological fluids, was found to form ion-pairs as demonstrated by its ability to partition into 1-butanol from acidic solutions. A similar relationship was observed for the effect of acids on the absorption of intraduodenally and orally administered solutions of mixidine in rats (as determined by lethality). Studies also demonstrated that the pH-lethality effects were not specific for a particular counterion. Mixidine was more lethal when administered intraduodenally than when administered orally,

and the counterions *per se* were not lethal in the doses used.

Keyphrases □ Mixidine—ion-pair formation *in vitro* determined by partitioning, absorption in rats determined by lethality □ Ion-pair formation—mixidine *in vitro*, determined by partitioning □ Absorption—mixidine in rats, determined by lethality □ Vasodilators, coronary—mixidine, ion-pair formation *in vitro* determined by partitioning, absorption in rats determined by lethality

The utilization of ion-pairs, neutral species formed by electrostatic attraction between oppositely charged ions in solution, has been studied as a method for improving drug absorption. The duration of rabbit corneal anesthesia was related to the chloroform–water distribution of di-

bucaine combined with 10 counterion species (1). The enhanced pharmacological effect of an orally administered quaternary ammonium compound by trichloroacetic acid was related to increases in partition between chloroform or 1-octanol and pH 6 buffer (2).